Supporting Information for

In vivo targeted magnetic resonance imaging and visualized photodynamic therapy in deep-tissue cancers using folic acid-functionalized superparamagnetic-upconversion nanocomposites

Leyong Zeng[a,b], Lijia Luo[a], Yuanwei Pan[a], Song Luo[b], Guangming Lu[b,c,*], Aiguo Wu[a,*]

a Key Laboratory of Magnetic Materials and Devices & Division of Functional Materials and Nanodevices, Ningbo Institute of Materials Technology and Engineering, Chinese Academy of Sciences, Ningbo 315201, P. R. China.. Fax: 86 574 86685163; Tel: 86 574 86685039; E-mail: aiguo@nimte.ac.cn

b Department of Medical Imaging, Jinling Hospital, School of Medicine, Nanjing University, Nanjing 210002, P. R. China.. Fax: 86 25 84804659; Tel: 86 25 80860185; E-mail: cjr.luguangming@vip.163.com

c State Key Laboratory of Analytical Chemistry for Life Science, School of Chemistry and Chemical Engineering, Nanjing University, Nanjing 210093, P.R. China.

1. Detailed Synthesis of Nanocomposites

Firstly, core-shell Fe_3O_4-$NaYF_4$:Yb/Er nanoparticles (NPs) were prepared following the previous reported method [1]. Secondly, the as-prepared NPs were modified by PEG and APTS, respectively. Briefly, 1 g of PEG was mixed with 1 mmol of NPs in 100 mL of ethanol, was stirred for 24 h, and washed in ethanol for three times. Then 0.5 mL of APTS in 10 mL ethanol was added into the above NPs in 90 mL of ethanol, was stirred for another 24 h, and washed in water for three times. Thirdly, 0.1 mmol of EDC and 0.1 mmol of NHS were dissolved in 10 mL of water, and then dropped into 50 mL of 10 mmol/L NH_2-NPs. 0.05 mmol of natrium folicum (FA-Na, obtained by reaction of FA and NaOH) was added into the above solution under continuous stirring. After 24 h, the obtained FA-targeted NPs (FA-NPs) were collected by centrifugation, and washed in water for three times, and were re-dispersed in 50 mL of water.

Finally, 1 mL of 1 mg/mL $AlPcS_4$ photosensitizers was added into 20 mL of 5 mg/mL FA-NPs, and was stirred in dark. After 24 h, the obtained PS-loaded FA-NPs (FA-NPs-PS) were collected by centrifugation, and washed in water for three times, and were re-dispersed in 20 mL of water.

2. Cell Culture, Cytotoxicity and Cellular Uptake

Human breast cancer cells (MCF-7) and human cervical cancer cells (HeLa) were cultured in DMEM culture medium supplemented with 10 % of fetal bovine serum, 100 units/mL of penicillin and 100 mg/mL of streptomycin at 37 ^oC in 5 % CO_2. MCF-7 and HeLa cells in logarithmic growth were cultured for 24 h, then incubated with 100 μg/mL FA-NPs-PS for another 12 h, and the cellular uptakes of FA-NPs-PS in MCF-7 and HeLa cells were characterized by a transmission electron microscope operated at 100 kV, respectively.

Alternatively, MCF-7 and MCF-7/ADR cells in logarithmic growth were cultured in 96-well plates for 24 h, and then incubated with NPs, FA-NPs, NP-PS, FA-NPs-PS for another 48 h, respectively. The concentrations of different nanoparticles were 0, 50, 100, 150, 200, and 250 μg/mL. Finally, the viabilities of MCF-7 and HeLa cells were measured by MTT assay, and the PS fluorescence imaging was also characterized by an animal imaging system.

3. Animal Models and *in Vivo* Biocompatibility

Female Balb/c (nu/nu) nude mice (18-20 g, 4-6 weeks old) were used in this work. All the experimental protocols involving animals were approved by the Institutional Animal Care and Use Committee of Jinling Hospital, and all the mice received humane care in compliance with the guide for the Care and Use of Laboratory Animals. Moreover, the experiments in the present study were performed in the Animal Centre of Jinling Hospital. In this work, MCF-7-tumor-bearing nude mice model was established and used in MRI and PDT. Briefly, MCF-7 cells were diluted with PBS and then injected subcutaneously to each mouse at the back with about 1×10^7 cells. When the tumors grew to be about 50-100 mm^3, the *in vivo* therapy was carried out.

For biocompatibility measurement, 18-20g healthy nude mice (4-6 weeks old) were injected with 100 μL of PBS and FA-NPs-PS (500 μg/mL in PBS) via tail vein, respectively. After 15 days, they were sacrificed, and the major organs of heart, liver, spleen, lung, kidney, and intestine were dissected for H&E staining.

4. Zeta Potentials of different nanocomposites

The Zeta potential was measured by Malvern Zetasizer Nanoseries. As shown in **Figure S1**, the Zeta potentials of NPs, FA-NPs, and FA-NPs-PS were 37.1 mV, 16.8 mV and 12.5 mV, respectively.

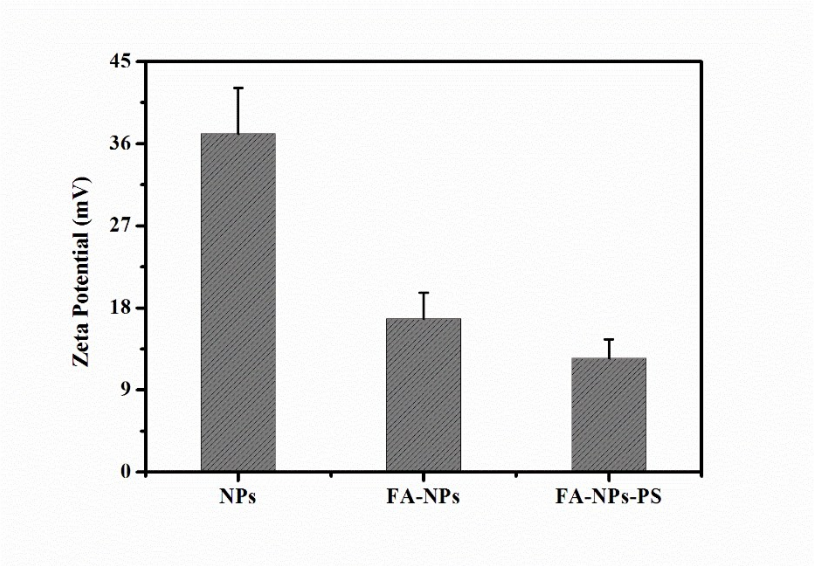

Figure S1 Zeta potential of NPs, FA-NPs and FA-NPs-PS.

5. UV-vis Absorption Spectra of different Materials

To investigate the effect of FA conjugation and PS loading on UV-vis spectra, the UV-vis spectra of free FA, free PS, NPs/NPs-PS and FA-NPs/FA-NPs-PS were measured, as shown in **Figure S2 and S3**.

In **Figure S2**(a), a wind absorbance band located at about 330-400 nm could be observed in UV-vis spectrum of free FA. Moreover, three main peaks were observed in UV-vis spectrum of free PS, which were located at about 670 nm, 630 nm and 350 nm, respectively, as shown in **Figure S2**(b). In order to further confirm the origin of wide band at about 380 nm, the UV-vis

spectra NPs and NPs-PS showed no wide bands at about 380 nm, but only peaks (at about 670 nm, 630 nm and 350 nm) appeared in NPs-PS (**Figure S3**(a)). However, in UV-vis spectra of FA-NPs and FA-NPs-PS, wind bands at about 380 nm were observed, and the band was winder in FA-NPs-PS, which could attributed to the peak overlap of FA and PS (**Figure S3**(b)).

Therefore, based on the results of **Figure S2** and **Figure S3**, it could be concluded that the wide absorbance bands at about 380 nm in FA-NPs-PS could be attributed to FA.

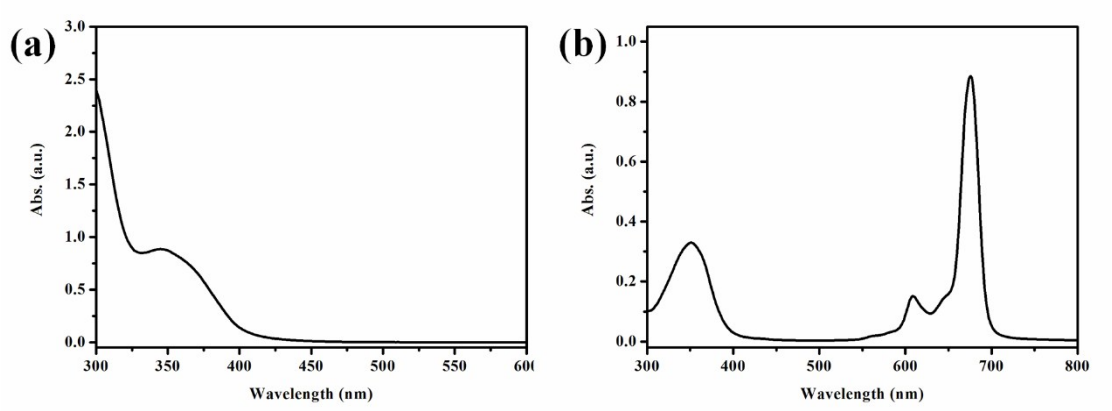

Figure S2 UV-vis absorption spectra of free FA and PS. (a) free FA; (b) free PS.

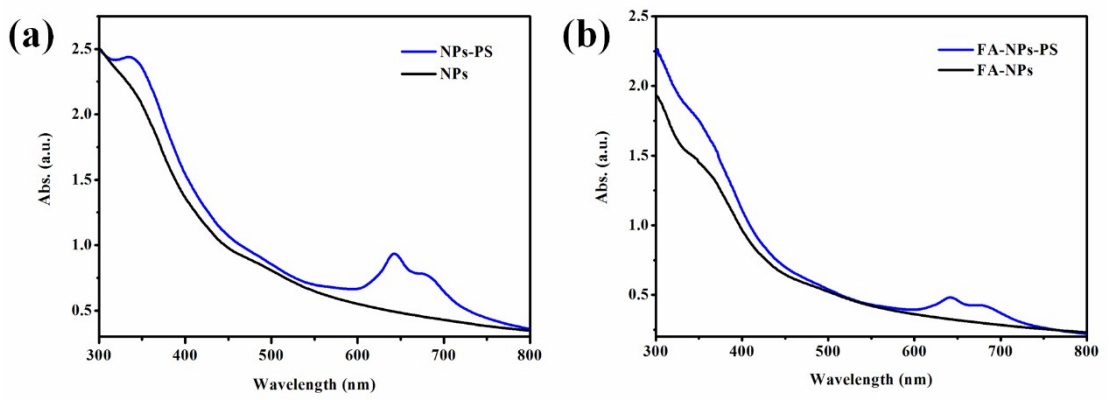

Figure S3 UV-vis absorption spectra of different nanocomposites. (a) NPs and NPs-PS; (b) FA-NPs and FA-NPs-PS.

7. Flow Cytometer Assay of MCF-7 and HeLa Cells Incubated with Different Nanocomposites

In order to quantitatively characterize the targeting ability of FA, the flow cytometer assay of MCF-7 cells and HeLa cells incubated with NPs-PS and FA-NPs-PS nanocomposites was

measured by detecting PS fluorescence. As shown in **Figure S4** and **Figure S5**, the fluorescence of PS was greatly enhanced in MCF-7 and HeLa cells incubated with FA-NPs-PS than that of NPs-PS. The results also suggested that FA-targeted FA-NPs-PS nanocomposites greatly promoted the uptakes of PS in MCF-7 and HeLa cells.

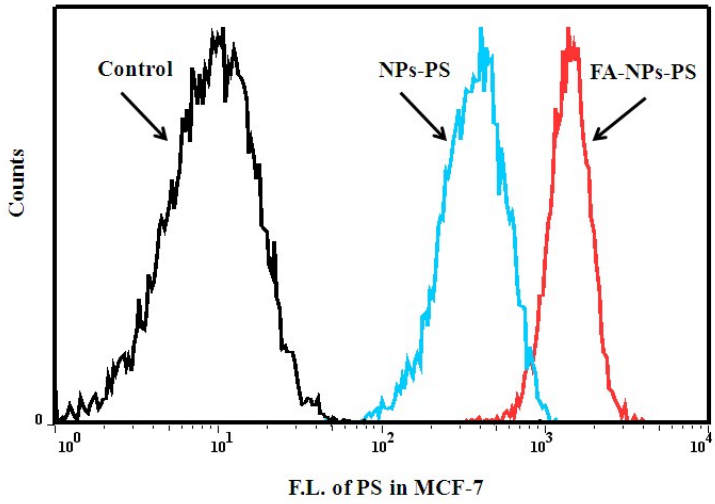

Figure S4 Flow cytometer curves of MCF-7 cells incubated with NPs-PS and FA-NPs-PS nanocomposites.

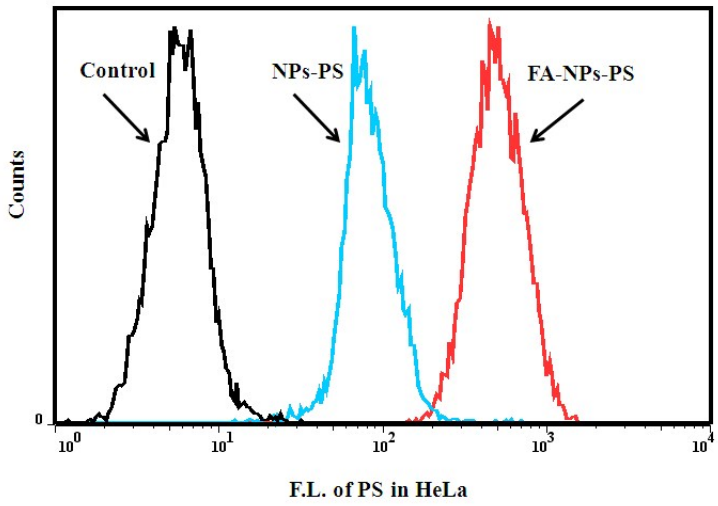

Figure S5 Flow cytometer curves of HeLa cells incubated with NPs-PS and FA-NPs-PS nanocomposites.

8. *In Vivo* Biodistribution of FA-NPs-PS nanocomposites

In order to quantitatively investigate the *in vivo* targeting ability, the *in vivo* biodistribution

of nanocomposites (in tumor, heart, liver, spleen, lung and kidney) through intravenous injection (in 3 mice) was measured by ICP-MS. As shown in **Figure S6**, the average concentration of nanocomposites (by measuring Y element) in liver, spleen, heart, lung, kidney and tumor was 4.41, 7.12, 0.13, 0.54, 0.39 and 0.95 μg/g, respectively, which indicated that FA-NPs-PS nanocomposites could be accumulated more in tumor, except in liver and spleen.

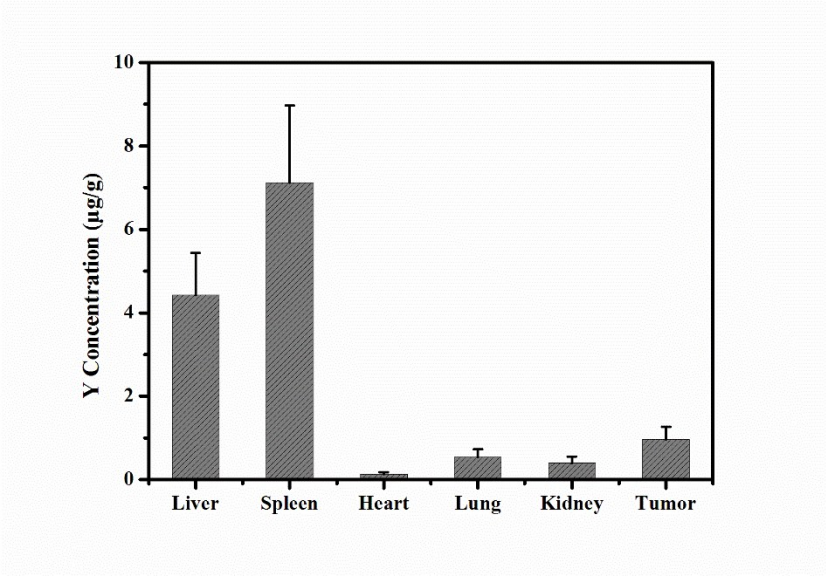

Figure S6 Biodistribution of FA-NPs-PS nanocomposites in tumor and major organs of MCF-7 tumor-bearing nude mice at 24 h after intravenous injection.

Reference

1. L. Zeng, L. Xiang, W. Ren, J. Zheng, T. Li, B. Chen, J. Zhang, C. Mao, A. Li and A. Wu, *RSC. Adv.*, 2013, **3**, 13915-13925.